Time evolution equation for advective heat transport as a constraint for optimal bounds in Rayleigh-Bénard convection

A. Tilgner
Institute of Geophysics, University of Göttingen, Friedrich-Hund-Platz 1, 37077 Göttingen, Germany

(Received 12 October 2018; published 14 January 2019)

Upper bounds on the heat transport and other quantities of interest in Rayleigh-Bénard convection are derived in previous work from constraints resulting from the equations of time evolution for kinetic energy, the root mean square of temperature, and the temperature averaged over horizontal planes. Here we investigate the effect of a constraint derived from the time evolution equation for the advective heat transport. This additional constraint leads to improved bounds on the toroidal dissipation.

DOI: 10.1103/PhysRevFluids.4.014601

I. INTRODUCTION

Thermal convection is among the best studied problems of fluid mechanics. Its most basic idealization is Rayleigh-Bénard convection in which a fluid fills a plane layer infinitely extended in the horizontal directions, heated from below and cooled from above. The applied temperature difference, or the amplitude of the driving of the flow, is commonly expressed in terms of the Rayleigh number. Numerical simulations and experiments can investigate convection only up to a certain Rayleigh number. It is also possible to derive rigorous bounds on, for example, the heat transport across the convecting layer [1–5]. The bounds derived in these references are valid at all Rayleigh numbers, but they tend to overestimate the actual heat transport. If power laws are fitted to both the bounds and numerically computed time averages, the fit to the bounds has a larger prefactor and usually a larger exponent. Furthermore, the bounds do not show any Prandtl number dependence.

These deficiencies arise because the derivation of the bounds does not exploit the full equations of evolution but only a few integrals deduced from them: the energy budget, the relation between advective heat transport and dissipation, and the temperature equation integrated over horizontal planes. Seis [5] also makes use of the maximum principle for temperature. An improvement of the bounds necessarily requires one to take advantage of additional constraints. This process is already well understood for systems of ordinary differential equations such as the Lorenz model [6]. In the context of convection, the implementation of further constraints is more cumbersome. Vitanov and Busse [7] split the energy budget into two equations, one for the poloidal and one for the toroidal energy. The resulting optimization problem preserves a dependence on the Prandtl number (and also on rotation if one is interested in rotating convection). But there is a price to pay in this approach. The optimization problem is not convex, and its Euler-Lagrange equations have to be solved numerically. Because of extensive coupling between different modes in a spectral decomposition of these equations, a numerical solution can only be obtained at low resolution and hence at low Rayleigh numbers.

The approach pursued in this paper is to solve a semidefinite program (SDP). Previously obtained bounds on Rayleigh-Bénard convection can be reproduced by this method [8]. It has already been demonstrated how one can obtain increasingly sharp bounds on solutions of systems of ordinary differential equations by including more and more constraints [6,9]. While the same systematic procedure is in principle possible for the Navier-Stokes equation [10], it becomes unpractical for Rayleigh-Bénard convection even at modest Rayleigh numbers because all energy unstable modes need to be retained which leads to a large SDP. Fantuzzi *et al.* [11] study bounds for Bénard-Marangoni convection and in this context discuss in depth limitations of the SDP approach and possible future lines of investigation. At present, the most straightforward approach remains to formulate an optimization problem in the form of an SDP with many decoupled linear matrix inequalities rather than a problem with a few but large linear matrix inequalities. The goal of the present paper is to derive a Prandtl number-dependent optimization problem for Rayleigh-Bénard convection which is convex and whose solution does not imply a significantly larger computational burden than optimization problems solved previously to find bounds on various observables of interest in Rayleigh-Bénard convection.

II. THE OPTIMIZATION PROBLEM

Let us consider the problem of Rayleigh-Bénard convection within the Boussinesq approximation for stress-free boundaries. This choice of boundary conditions is not essential for obtaining the constraint, but it simplifies the calculation. A Cartesian coordinate system (x, y, z) is chosen such that a plane layer is infinitely extended in the x and y directions, and the boundaries of the layer are separated by the distance h along the z direction. Gravitational acceleration g is acting along the negative z direction. The layer is filled with fluid of density ρ, kinematic viscosity ν, thermal diffusivity κ, and thermal expansion coefficient α. Top and bottom boundaries are held at the fixed temperatures T_{top} and $T_{\text{top}} + \Delta T$, respectively. We will consider the equations of evolution immediately in nondimensional form, choosing for units of length, time, and temperature deviation from T_{top} the quantities h, h^2/κ, and ΔT. With this choice, the equations within the Boussinesq approximation for the fields of velocity $\boldsymbol{v}(\boldsymbol{r}, t)$, temperature $T(\boldsymbol{r}, t)$, and pressure $p(\boldsymbol{r}, t)$ become

$$\frac{1}{\text{Pr}}(\partial_t \boldsymbol{v} + \boldsymbol{v} \cdot \nabla \boldsymbol{v}) = -\nabla p + \text{Ra}\theta \hat{\boldsymbol{z}} + \nabla^2 \boldsymbol{v}, \tag{1}$$

$$\partial_t \theta + \boldsymbol{v} \cdot \nabla \theta - v_z = \nabla^2 \theta, \tag{2}$$

$$\nabla \cdot \boldsymbol{v} = 0. \tag{3}$$

In these equations, $T = \theta + 1 - z$, so that θ represents the deviation from the conduction profile. The Prandtl number Pr and the Rayleigh number Ra are given by

$$\text{Pr} = \frac{\nu}{\kappa}, \quad \text{Ra} = \frac{g\alpha \Delta T h^3}{\kappa \nu}, \tag{4}$$

and $\hat{\boldsymbol{z}}$ denotes the unit vector in z direction. The boundary conditions on temperature require that $\theta = 0$ at $z = 0$ and 1, and the stress-free conditions chosen here lead to $\partial_z v_x = \partial_z v_y = v_z = 0$ at the boundaries.

It will be helpful to reduce the number of dependent variables by introducing poloidal and toroidal scalars ϕ and ψ such that $\boldsymbol{v} = \nabla \times \nabla \times (\phi \hat{\boldsymbol{z}}) + \nabla \times (\psi \hat{\boldsymbol{z}})$ and $\nabla \cdot \boldsymbol{v} = 0$ is satisfied by construction. The z component of the curl and the z component of the curl of the curl of Eq. (1) yield the equations of evolution for ϕ and ψ,

$$\frac{1}{\text{Pr}}\{\partial_t \nabla^2 \Delta_2 \phi + \hat{\boldsymbol{z}} \cdot \nabla \times \nabla \times [(\nabla \times \boldsymbol{v}) \times \boldsymbol{v}]\} = \nabla^2 \nabla^2 \Delta_2 \phi - \text{Ra} \Delta_2 \theta, \tag{5}$$

$$\frac{1}{\text{Pr}}\{\partial_t \Delta_2 \psi - \hat{\boldsymbol{z}} \cdot \nabla \times [(\nabla \times \boldsymbol{v}) \times \boldsymbol{v}]\} = \nabla^2 \Delta_2 \psi, \tag{6}$$

with $\Delta_2 = \partial_x^2 + \partial_y^2$. For brevity, $\boldsymbol{v}$ is not replaced by its expression in terms of ϕ and ψ in these equations. The stress-free boundary conditions translate into $\phi = \partial_z^2 \phi = \partial_z \psi = 0$.

The currently known methods for obtaining upper bounds on fluid dynamic quantities cannot exploit the equations of evolution in full detail but extract averages from the original equations.

Several types of averages will become important: the average over the entire volume, denoted by angular brackets without subscript, the average over an arbitrary plane $z = \text{const}$, denoted by $\langle \cdots \rangle_A$, and the average over time, which will be signaled by an overline.

Three useful relations between averages can now directly be obtained. The average of Eq. (2) over planes $z = \text{const}$ leads to

$$\partial_t \langle \theta \rangle_A = \langle \partial_z (\theta \Delta_2 \phi) \rangle_A + \left\langle \partial_z^2 \theta \right\rangle_A. \tag{7}$$

Multiplication of Eq. (2) with θ and a subsequent volume average yields

$$\partial_t \left\langle \frac{1}{2} \theta^2 \right\rangle = -\langle \theta \Delta_2 \phi \rangle - \langle |\nabla \theta|^2 \rangle. \tag{8}$$

Finally, the dot product of $\boldsymbol{v}$ with Eq. (1), followed by a volume average, leads to

$$\partial_t \left\langle \frac{1}{2} \boldsymbol{v}^2 \right\rangle = -\text{PrRa} \langle \theta \Delta_2 \phi \rangle - \text{Pr} \langle |(\hat{\boldsymbol{z}} \times \boldsymbol{\nabla}) \nabla^2 \phi|^2 + |\nabla \partial_x \psi|^2 + |\nabla \partial_y \psi|^2 \rangle. \tag{9}$$

These three equations form the basis of the previous work on bounds on, for instance, the Nusselt number Nu given by $\text{Nu} = 1 - \langle \overline{\theta \Delta_2 \phi} \rangle = 1 + \langle \overline{v_z \theta} \rangle$.

An additional relation will be derived below by computing $\partial_t \langle v_z \theta \rangle$ from the time evolution equation of the advective heat transport $v_z \theta$. There are at least two reasons why such a relation looks promising. Bounds have been computed for double diffusive convection. In this problem, salinity S drives convection together with temperature, and salinity obeys the same advection-diffusion equation as temperature except for a different diffusion constant. This problem looks superficially identical to ordinary convection, and one may think that adding the equation for $\partial_t \langle \frac{1}{2} S^2 \rangle$ to Eqs. (7)–(9) provides us with enough information to derive bounds on double diffusive convection. In fact, it does not. It is necessary to include the equation for $\partial_t \langle \theta S \rangle$ to derive bounds [12]. This demonstrates the usefulness of considering cross-products of different physical quantities and motivates us to also look at $\partial_t \langle v_z \theta \rangle$. Another type of flow to which bounding methods were applied in the past are flows in periodic volumes driven by a body force $\boldsymbol{f}$ [13–16]. In these problems, it is essential to include the equation for $\partial_t \langle \boldsymbol{f} \cdot \boldsymbol{v} \rangle$ obtained by forming the dot product of the momentum equation with $\boldsymbol{f}$. In Rayleigh-Bénard convection, the buoyancy force plays the role of the body force in the momentum equation. From this analogy, we have another reason to look at $\partial_t \langle v_z \theta \rangle$.

If we multiply the z component of Eq. (1) by θ, Eq. (2) by v_z, add the two equations, and average the sum over the volume, we obtain the time evolution equation for the advective heat transport:

$$\partial_t \langle v_z \theta \rangle = \left\langle v_z^2 \right\rangle + \text{PrRa} \langle \theta^2 \rangle - (1 + \text{Pr}) \langle \boldsymbol{\nabla} \theta \cdot \boldsymbol{\nabla} v_z \rangle - \langle \theta \partial_z p \rangle. \tag{10}$$

Thanks to the stress-free boundary conditions and the boundary condition on temperature, one deduces from Eq. (1) that $\partial_z p = 0$ at the boundaries. The divergence of Eq. (1) yields $\nabla^2 p = -\boldsymbol{\nabla} \cdot [(\boldsymbol{v} \cdot \boldsymbol{\nabla}) \boldsymbol{v}] + \text{PrRa} \partial_z \theta$. It is therefore possible to split the pressure p into two terms p_1 and p_2 such that $p = p_1 + p_2$ and

$$\nabla^2 p_1 = -\boldsymbol{\nabla} \cdot [(\boldsymbol{v} \cdot \boldsymbol{\nabla}) \boldsymbol{v}], \tag{11}$$

$$\nabla^2 p_2 = \text{PrRa} \partial_z \theta, \tag{12}$$

with the boundary conditions that $\partial_z p_1 = \partial_z p_2 = 0$ at $z = 0$ and 1.

It will now be shown that the expression $\langle \theta \partial_z p_2 \rangle$ is quadratic in θ and positive. To this end, we first consider a layer with periodic boundary conditions and finite periodicity length in the lateral directions. At the end of the calculation, we will send the periodicity length to infinity in order to obtain the desired result for the infinitely extended layer. It helps to introduce two functions f and g defined by $f = \partial_z p_2 / (\text{PrRa})$ (so that $\nabla^2 f = \partial_z^2 \theta$) and $\nabla^2 g = \theta$ with the boundary conditions

$g = 0$ at $z = 0$ and 1. These definitions imply that f and g are periodic in x and y and that $f = \partial_z^2 g = g = 0$ at $z = 0$ and 1. It is possible to compute $\int \theta \partial_z p_2 \, dV$, where the integration extends over the volume V of a periodicity cell in the layer, by a sequence of integration by parts in which the boundary integrals all vanish:

$$\frac{1}{\mathrm{PrRa}} \int \theta \partial_z p_2 \, dV = \int (\nabla^2 g) f \, dV = \int g (\nabla^2 f) \, dV = \int g \partial_z^2 \nabla^2 g \, dV$$
$$= -\int (\partial_z g)(\partial_z \nabla^2 g) \, dV = \int |\partial_z \nabla g|^2 \, dV. \tag{13}$$

We can now divide this equation by the volume V and take the limit $V \to \infty$ to conclude that

$$\langle \theta \partial_z p_2 \rangle = \mathrm{PrRa} \langle |\partial_z \nabla \Delta^{-1} \theta|^2 \rangle, \tag{14}$$

where Δ^{-1} denotes the inverse Laplacian for homogeneous Dirichlet boundary conditions.

Before proceeding further, let us look at the form of the optimization problem which yields optimal bounds from Eqs. (7)–(10). There are various ways to formulate such an optimization problem. The formulation presented here is most closely related to the method of auxiliary functions [6,10,17]. To facilitate the exposition of the numerical implementation later, the formulation presented here is identical to Ref. [8]. Suppose we want to bound some objective function Z which is defined in terms of the velocity and temperature fields. We chose test functions $\varphi_n(z), n = 1, \dots, N$, which depend only on z and on which we project Eq. (2):

$$\partial_t \langle \varphi_n \theta \rangle = \langle \varphi_n \partial_z (\theta \Delta_2 \phi) \rangle + \langle \varphi_n \nabla^2 \theta \rangle. \tag{15}$$

We now construct the functional $F(\lambda_1, \dots, \lambda_N, \lambda_R, \lambda_E, \lambda_M, \theta, \phi, \psi)$ as

$$F(\lambda_1, \dots, \lambda_N, \lambda_R, \lambda_E, \lambda_M, \theta, \phi, \psi) = \sum_{n=1}^{N} \lambda_n \partial_t \langle \varphi_n \theta \rangle - \lambda_R \partial_t \left\langle \frac{1}{2} \theta^2 \right\rangle - \frac{\lambda_E}{\mathrm{Pr}} \partial_t \left\langle \frac{1}{2} \boldsymbol{v}^2 \right\rangle + \lambda_M \partial_t \langle v_z \theta \rangle \tag{16}$$

and replace all time derivatives by their expressions given in Eqs. (8), (9), (15), and (10). The task now is to find a set of coefficients $\lambda_0, \lambda_1, \dots, \lambda_N, \lambda_R, \lambda_E, \lambda_M$ such that the inequality

$$-Z + \lambda_0 + F(\lambda_1, \dots, \lambda_N, \lambda_R, \lambda_E, \lambda_M, \theta, \phi, \psi) \geqslant 0 \tag{17}$$

holds for all fields $\theta(\boldsymbol{r})$, $\phi(\boldsymbol{r})$, and $\psi(\boldsymbol{r})$ which obey the free slip boundary conditions and $\theta = 0$ at $z = 0$ and 1. If such a set of λ's is found, the above inequality holds in particular for the fields taken from an actual time evolution. Taking the time average of relation (17) thus leads to $\overline{Z} \leqslant \lambda_0 - \overline{F} = \lambda_0$. The time average of F is zero because it is the linear combination of time derivatives. Replacing the time derivatives by their expressions in Eqs. (8), (9), (15), and (10), the best upper bound for $\overline{Z}$ is given by the λ_0 which solves the optimization problem

$$\begin{aligned}
&\text{minimize} \quad \lambda_0, \\
&\text{subject to} \quad -Z + \lambda_0 + \sum_{n=1}^{N} \lambda_n [\langle \varphi_n \partial_z (\theta \Delta_2 \phi) \rangle + \langle \varphi_n \nabla^2 \theta \rangle] + \lambda_R [\langle \theta \Delta_2 \phi \rangle + \langle |\nabla \theta|^2 \rangle] \\
&\quad + \lambda_E [\mathrm{Ra} \langle \theta \Delta_2 \phi \rangle + \langle |(\hat{\boldsymbol{z}} \times \nabla) \nabla^2 \phi|^2 \rangle + d^2] + \lambda_M \big[\langle v_z^2 \rangle + \mathrm{PrRa}(\langle \theta^2 \rangle - \langle |\partial_z \nabla \Delta^{-1} \theta|^2 \rangle) \\
&\quad - (1 + \mathrm{Pr}) \langle \nabla \theta \cdot \nabla v_z \rangle - \langle \theta \partial_z p_1 \rangle \big] \geqslant 0,
\end{aligned} \tag{18}$$

with $d^2 = \langle |\nabla \partial_x \psi|^2 + |\nabla \partial_y \psi|^2 \rangle$. The minimization occurs over all λ's and the inequality needs to hold for all d and all eligible θ and ϕ.

This is nearly in a form which leads to an SDP after a suitable discretization. The problematic term is $\langle \theta \partial_z p_1 \rangle$, which involves a triple product in terms of θ, ϕ, and ψ. However, this term is readily reduced to a quadratic term by invoking the maximum principle, which guarantees that in a statistically stationary state, the temperature takes on values in the interval bounded by the temperatures at the top and bottom planes of the layer, which means that $0 \leqslant T = \theta + 1 - z \leqslant 1$, or equivalently, $|T - \frac{1}{2}| \leqslant \frac{1}{2}$.

To make best use of the maximum principle, we want to compute $\langle \theta \partial_z p_1 \rangle$ in the form $\langle (T - \frac{1}{2})\partial_z p_1 \rangle + \langle (z - \frac{1}{2})\partial_z p_1 \rangle$. This expression can be simplified with the same artifice as before: we first integrate over a volume V with periodic boundary conditions in the horizontal before taking the limit $V \to \infty$. The second term of the above expression requires us to compute

$$\int \left(z - \frac{1}{2}\right)\partial_z p_1 \, dV = \int dz \left(z - \frac{1}{2}\right)\partial_z \iint dx\, dy\, p_1, \tag{19}$$

in which only the horizontal average of p_1 appears, which obeys

$$\begin{aligned}\iint dx\, dy\, \nabla^2 p_1 &= \iint dx\, dy\, \partial_z^2 p_1 = -\iint dx\, dy\, \nabla \cdot [(\boldsymbol{v} \cdot \nabla)\boldsymbol{v}] \\ &= -\partial_z \iint dx\, dy\, \nabla(\boldsymbol{v} v_z) = -\partial_z^2 \iint dx\, dy\, v_z^2. \end{aligned} \tag{20}$$

We can thus solve $\partial_z^2 \iint dx\, dy \partial_z p_1 = -\partial_z^2 \iint dx\, dy v_z^2$ with the boundary conditions that $\iint dx\, dy\, \partial_z p_1 = 0$ at $z = 0$ and 1 to find $\iint dx\, dy\, \partial_z p_1 = -\iint dx\, dy\, v_z^2$ since $v_z = 0$ at $z = 0$ and 1. Inserting this into Eq. (19) yields

$$\int \left(z - \frac{1}{2}\right)\partial_z p_1 \, dV = -\int dz \left(z - \frac{1}{2}\right)\partial_z \iint dx\, dy\, v_z^2 = \int v_z^2 \, dV \tag{21}$$

after another integration by parts.

The only triple product left in problem (18) is $\lambda_M \langle \theta \partial_z p_1 \rangle$. This can be reduced to a quadratic term only at the price of an inequality:

$$\lambda_M \int \left(T - \frac{1}{2}\right)\partial_z p_1 \, dV \leqslant |\lambda_M| \int \left|T - \frac{1}{2}\right| \cdot |\partial_z p_1| \, dV \leqslant \frac{1}{2}|\lambda_M| \int |\partial_z p_1| \, dV. \tag{22}$$

The last expression is quadratic in $\boldsymbol{v}$ and could be combined with (18) to obtain a convex optimization problem which can be represented as an SDP for numerical purposes. However, the solution of this problem would be very expensive. The success of the previous applications of semidefinite programming to Rayleigh-Bénard convection [8] relied on the fact that if the dependence in x and y is represented as Fourier series, the equations decouple in the wave number of the Fourier modes and only a small number of amplitudes of Fourier modes needs to be taken into account in a numerical computation. The term $\int |\partial_z p_1| dV$ unfortunately destroys that decoupling.

The decoupling can be restored at the expense of a further inequality. It is shown in the Appendix that

$$\langle |\partial_z p_1| \rangle \leqslant \frac{1}{2}\left\langle \sum_{i,j} (\partial_i v_j)^2 \right\rangle. \tag{23}$$

Inserting this into Eq. (22), and (22) together with (21) into (18), leads to the following optimization problem for the optimal bound λ_0 of the objective function $\overline{Z}$, where the minimum is sought over all λ's:

$$\begin{aligned} &\text{minimize} \quad \lambda_0, \\ &\text{subject to} \quad -Z + \lambda_0 + \sum_{n=1}^{N} \lambda_n [\langle \varphi_n \partial_z(\theta \Delta_2 \phi) \rangle + \langle \varphi_n \nabla^2 \theta \rangle] + \lambda_R[\langle \theta \Delta_2 \phi \rangle + \langle |\nabla \theta|^2 \rangle] \\ &\quad + \lambda_E[\mathrm{Ra}\langle \theta \Delta_2 \phi \rangle + \langle |(\hat{z} \times \nabla)\nabla^2 \phi|^2 \rangle + d^2] \end{aligned}$$

$$+\lambda_M[\mathrm{PrRa}(\langle\theta^2\rangle - \langle|\partial_z\nabla\Delta^{-1}\theta|^2\rangle) - (1+\mathrm{Pr})\langle\nabla\theta\cdot\nabla v_z\rangle] \geqslant \frac{1}{4}\lambda_{\mathrm{abs}}\left\langle\sum_{i,j}(\partial_i v_j)^2\right\rangle$$

$$\lambda_{\mathrm{abs}} \geqslant \lambda_M \geqslant -\lambda_{\mathrm{abs}}. \tag{24}$$

The last line implies $|\lambda_M| \leqslant \lambda_{\mathrm{abs}}$. Since the right-hand side of the first inequality constraint in (24) is positive, λ_0 is smallest when λ_{abs} is chosen as small as possible, which implies that $\lambda_{\mathrm{abs}} = |\lambda_M|$ at optimum. The velocity field is left as a variable in (24) so that it is easier to trace the various terms to the preceding development, but eventually, v_z is replaced by $v_z = -(\partial_x^2 + \partial_y^2)\phi$ and

$$\left\langle\sum_{i,j}(\partial_i v_j)^2\right\rangle = \langle|(\hat{z}\times\nabla)\nabla^2\phi|^2\rangle + d^2.$$

Problem (24) contains Eq. (10) as a constraint which keeps Pr as a parameter in the optimization. The effect of Pr is expected to be strongest for $\mathrm{Pr}\to\infty$. It will be of interest to also study a reduced optimization problem which results from (24) by introducing $\lambda'_M = \lambda_M\mathrm{Pr}$, $\lambda'_{\mathrm{abs}} = \lambda_{\mathrm{abs}}\mathrm{Pr}$. The dissipation is known to be bounded uniformly in Pr [1–3], so that in the limit $\mathrm{Pr}\to\infty$, the right-hand side of the inequality constraint disappears and we are left with a simpler problem:

$$\begin{aligned}
&\text{minimize} \quad \lambda_0,\\
&\text{subject to} \quad -Z + \lambda_0 + \sum_{n=1}^{N}\lambda_n[\langle\varphi_n\partial_z(\theta\Delta_2\phi)\rangle + \langle\varphi_n\nabla^2\theta\rangle] + \lambda_R[\langle\theta\Delta_2\phi\rangle + \langle|\nabla\theta|^2\rangle]\\
&\quad + \lambda_E[\mathrm{Ra}\langle\theta\Delta_2\phi\rangle + \langle|(\hat{z}\times\nabla)\nabla^2\phi|^2\rangle + d^2]\\
&\quad + \lambda'_M[\mathrm{Ra}(\langle\theta^2\rangle - \langle|\partial_z\nabla\Delta^{-1}\theta|^2\rangle) - \langle\nabla\theta\cdot\nabla v_z\rangle] \geqslant 0.
\end{aligned} \tag{25}$$

The virtue of this formulation is that it is independent of any sloppiness that may have eased the derivation of Eq. (23). The optimization (25) would not be changed by a sharper inequality than (23).

The numerical solution of problems (24) and (25) proceeds in exactly the same way as in Ref. [8] so that a brief summary will suffice here. The variables ϕ and θ are decomposed into N Chebychev polynomials T_n for the z direction and into plane waves in x and y, as, for example, in

$$\theta = \sum_{n=1}^{N}\sum_{k_x}\sum_{k_y}\hat{\theta}_{n,k_x,k_y}T_n(2z-1)e^{i(k_x x + k_y y)}. \tag{26}$$

The test functions φ_n are chosen as delta functions centered at the collocation points z_n defined by

$$z_n = \frac{1}{2}\left[1 + \cos\left(\pi\frac{n-1}{N-1}\right)\right], \quad n = 1,\ldots,N, \tag{27}$$

$$\varphi_n(z) = \delta(z - z_n). \tag{28}$$

Inserting all this into the optimization problems transforms the inequality constraints into the condition that some symmetric matrix be positive semidefinite. This is the standard form of an SDP. The constraints decouple in $k^2 = k_x^2 + k_y^2$. Only a small number of wave numbers actually constrain the solution. This set of wave numbers is determined automatically [8]. The matrix occurring in the SDP would be much larger if the constraints did not decouple in k, hence the effort put into obtaining Eq. (23). Some improvements of the basic method accelerate the computation but are not essential. These include a partial integration of Eq. (15) and the exploitation of symmetry in z [8]. The resulting SDP was solved with the package cvxopt.

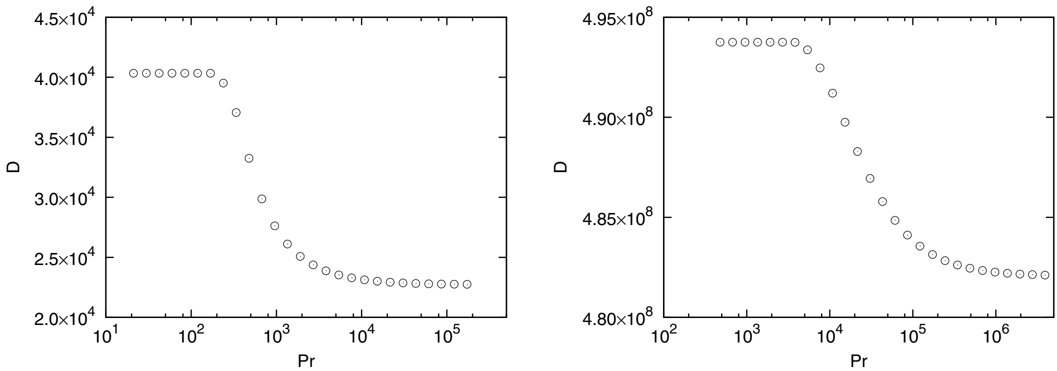

FIG. 1. The bound D as a function of Pr for Ra $= 1.6 \times 10^4$ (left panel) and 8.192×10^6 (right panel).

III. RESULTS

The optimization problem (24) distinguishes itself from previous problems by the terms multiplied by λ_M and λ_{abs}, which include all the terms containing Pr. In order to test the power of the constraint, it seems best to choose an objective function which varies dramatically as a function of Pr. The dissipation of the nonpoloidal components fulfills this criterion, because the flow is purely poloidal at infinite Pr, whereas it contains both poloidal and toroidal components at finite Pr. The choice $Z = d^2$ thus promises to be a gratifying objective function.

Call D the optimal λ_0 of problem (24) for $Z = d^2$. Figure 1 shows D as a function of Pr for different Ra. It is seen that D is constant for low Pr until it monotonically decreases as a function of Pr and asymptotes towards a value different from zero at high Pr. The optimization problem (24) thus is not powerful enough to show that the toroidal dissipation disappears at infinite Pr. Let us denote with D_0 the value of D at small Pr and with D_∞ the limiting value of D as Pr tends to infinity. D_0 and D_∞ are functions of Pr.

D_0 is equal to the upper bound one obtains without the constraint derived from $\partial_t \langle v_z \theta \rangle$, or with $\lambda_M = \lambda_{\text{abs}} = 0$ in (24). This bound is the same as the one computed in Ref. [8] and obeys approximately $D_0 = 0.021 \times \text{Ra}^{3/2}$ at high Ra. The constraint introduced in this paper becomes active and reduces the upper bound for Pr $>$ Pr_a. From plots like Fig. 1 one finds Pr_a as a function of Ra, which is shown in Fig. 2. Pr needs to be larger than $\text{Pr}_a = 1.18 \times \text{Ra}^{1/2}$ to obtain improved bounds.

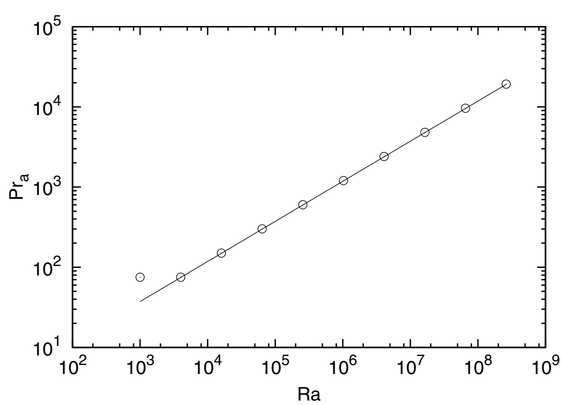

FIG. 2. The Prandtl number Pr_a that has to be exceeded for constraint (10) to reduce the bound D, plotted as function of Ra. The straight line is given by $1.18 \times \text{Ra}^{1/2}$.

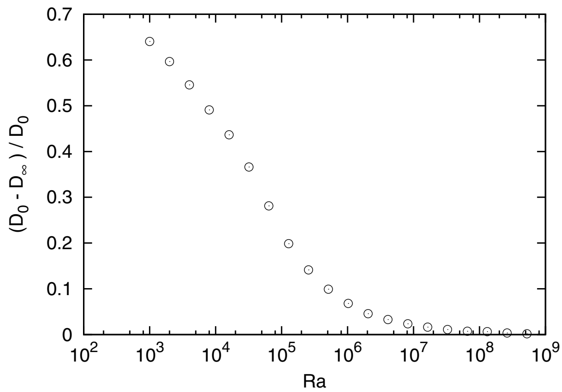

FIG. 3. $(D_0 - D_\infty)/D_0$ as a function of Ra.

Just as D_0 can be computed from a simplified optimization problem, so can D_∞ be computed from the reduced problem (25), which has the advantage that it does not depend on Pr anymore, and it is independent of how sharp the estimate in (23) is. $D_\infty(\mathrm{Ra})$ is the lowest bound found for any Pr at a given Ra, so that $(D_0 - D_\infty)/D_0$ is a measure of the maximum fractional improvement of the bound due to the additional constraint (10) at the given Ra. This fraction is shown in Fig. 3. As can be seen from this figure, the constraint (10) can improve the bound by more than a factor of 2 at small Ra, but dishearteningly, the improvement vanishes for large Ra. Bounding methods should be useful at high Ra when ordinary time integrations become too expensive. But it is precisely in this limit that the added constraint does not improve the previously known bound.

The objective function most often considered in the context of optimum theory is $Z = \langle v_z \theta \rangle$, which is the Nusselt number minus one. With this choice, the fractional improvement of previous known bounds is found to be less than 2×10^{-3}, and since this is less than the tolerances and errors in the numerical procedure, the improvement could be exactly zero. The potential improvement is at any rate so small that it was not considered worthwhile to determine it accurately, or to show that it vanishes.

IV. CONCLUSION

Previous work has derived bounds on the Nusselt number or other flow quantities in convection from the time evolution equations for $\langle \theta \rangle_A$, $\langle \frac{1}{2}\theta^2 \rangle$, and $\langle \frac{1}{2}\boldsymbol{v}^2 \rangle$. The present paper adds $\langle v_z \theta \rangle$ to the list. This additional constraint does not improve the bounds on the Nusselt number by an unambiguously detectable amount. The bounds on the toroidal dissipation on the other hand can be improved by more than 50%, but there is no improvement at large Ra. This fact is remarkable because it contradicts the behavior one may intuit from other results in the optimum theory of turbulence. In order to derive bounds for flows in three-dimensional (3D) periodic boxes driven by a body force $\boldsymbol{f}$, it is necessary to take into account the time evolution equation for $\langle \boldsymbol{f} \cdot \boldsymbol{v} \rangle$. For convection within the Boussinesq approximation, the momentum equation contains a driving term proportional to $\theta \hat{\boldsymbol{z}}$. The term analogous to $\langle \boldsymbol{f} \cdot \boldsymbol{v} \rangle$ of the 3D periodic box is therefore $\langle v_z \theta \rangle$. For an immediate analogy with previous work, the forcing should be solenoidal, so that we should first consider $\langle \boldsymbol{v} \cdot (\theta \hat{\boldsymbol{z}} - \boldsymbol{\nabla} \tilde{p}) \rangle$, where $\tilde{p}$ is chosen such that $\boldsymbol{\nabla} \cdot (\theta \hat{\boldsymbol{z}} - \boldsymbol{\nabla} \tilde{p}) = 0$. However, for a solenoidal velocity field with zero normal component at the boundaries, the expression $\langle \boldsymbol{v} \cdot (\theta \hat{\boldsymbol{z}} - \boldsymbol{\nabla} \tilde{p}) \rangle$ reduces to $\langle v_z \theta \rangle$. It is therefore surprising that there is not a more striking improvement of bounds for convective flows if the time evolution equation of $\langle v_z \theta \rangle$ is included in the optimization problem. At finite Pr, the bounding problem relies on inequality (23), which can possibly be improved. In the limit of large Pr, however, the results are independent of this inequality and no improvement of the results presented here can be achieved without adding yet another constraint.

APPENDIX

The goal of this appendix is to prove Eq. (23). To this end, we have to compute $\frac{1}{V}\int |\partial_z p_1|\, dV$, where V is an arbitrarily large volume in the plane layer, and p_1 is given by

$$\nabla^2 p_1 = q \tag{A1}$$

with $\partial_z p_1 = 0$ at $z = 0$ and 1. The variable q is used as an abbreviation for $q = -\nabla \cdot [(\boldsymbol{v} \cdot \nabla)\boldsymbol{v}]$. We will proceed by finding the Green's function $G(\boldsymbol{r}, \boldsymbol{r}')$ such that $\nabla^2 G(\boldsymbol{r}, \boldsymbol{r}') = \delta(\boldsymbol{r} - \boldsymbol{r}')$ so that $p_1(\boldsymbol{r}) = \int G(\boldsymbol{r}, \boldsymbol{r}')q(\boldsymbol{r}')\, d^3\boldsymbol{r}'$ where the integral extends over the horizontally infinitely extended layer. Once the Green's function is known, we can estimate the desired integral from

$$\begin{aligned}\frac{1}{V}\int |\partial_z p_1|\, dV &= \frac{1}{V}\int d^3\boldsymbol{r}\left|\int d^3\boldsymbol{r}'\partial_z G(\boldsymbol{r}, \boldsymbol{r}')q(\boldsymbol{r}')\right| \leqslant \frac{1}{V}\int d^3\boldsymbol{r}\int d^3\boldsymbol{r}'|\partial_z G(\boldsymbol{r}, \boldsymbol{r}')|\cdot|q(\boldsymbol{r}')| \\ &\leqslant \frac{1}{V}\int d^3\boldsymbol{r}'|q(\boldsymbol{r}')|\cdot \max_{\boldsymbol{r}'}\int d^3\boldsymbol{r}|\partial_z G(\boldsymbol{r}, \boldsymbol{r}')|\end{aligned} \tag{A2}$$

and taking the limit $V \to \infty$:

$$\langle|\partial_z p_1|\rangle \leqslant \langle|q|\rangle \cdot \max_{\boldsymbol{r}'}\int d^3\boldsymbol{r}|\partial_z G(\boldsymbol{r}, \boldsymbol{r}')|. \tag{A3}$$

Because of the translational invariance, the last factor in Eq. (A3) simplifies to

$$\max_{z'}\int d^3\boldsymbol{r}\left|\partial_z G\left(\boldsymbol{r}, \begin{pmatrix}0\\0\\z'\end{pmatrix}\right)\right|. \tag{A4}$$

The Green's function for Eq. (A1) with Neumann boundary conditions describes, for example, the potential flow out of a point source in a plane layer. The maximization in expression (A4) asks for the distance z' from the lower boundary of the layer at which one has to place the point source so that the absolute value of the z component of the velocity integrated over the entire layer is maximum. One intuitively expects that the maximum is reached when the point source is located on one of the boundaries of the layer. It seems very likely that the Green's function for exactly this problem is given somewhere in the existing literature, but I was not able to find a suitable reference. However, the Green's function for Eq. (A1) with the Dirichlet boundary conditions $p_1 = 0$ at $z = 0$ and 1 describes the electrostatic potential of a point charge between two parallel infinitely extended metallic plates kept at zero potential, and the Green's function for this electrostatic problem can be found in the textbook by Jackson [18]. Adapting the result in this textbook from Dirichtlet to Neumann boundary conditions leads to

$$G\left(\boldsymbol{r}, \begin{pmatrix}0\\0\\z'\end{pmatrix}\right) = \frac{1}{2\pi}\ln s - \frac{1}{\pi}\sum_{n=1}^{\infty} K_0(n\pi s)\cos(n\pi z)\cos(n\pi z') + C, \tag{A5}$$

where the position $\boldsymbol{r}$ is given in cylindrical coordinates (s, φ, z) and C is a constant left unspecified by the Neumann boundary conditions and which is irrelevant because we are only interested in $\partial_z G$. K_0 is a modified Bessel function of the second kind in the usual notation.

We will abstain from formal proofs for two properties which we will deduce from numerical evaluation of Eq. (A5) and which match the intuition about G one may have from its interpretation as a potential flow out of a point source. The first observation concerns the z' at which the maximum in (A4) is realized. Figure 4 shows $\int d^3\boldsymbol{r}|\partial_z G|$ as a function of z' computed numerically from the first 40 terms of Eq. (A5). As expected, this integral is maximal for $z' = 0$ (or $z' = 1$ by symmetry). The value of the maximum is numerically close to $1/2$.

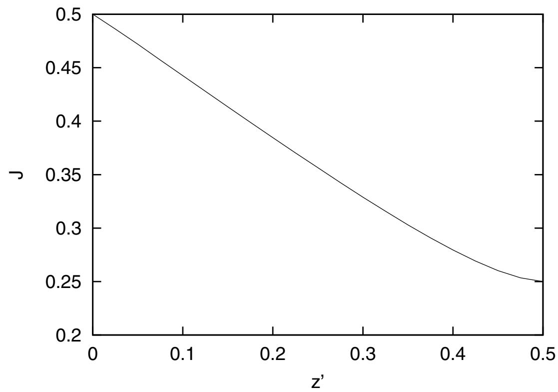

FIG. 4. The integral $J = \int d^3\boldsymbol{r}|\partial_z G(\boldsymbol{r},\boldsymbol{r}')|$ as a function of z', the z coordinate of $\boldsymbol{r}'$.

This second point can be made more precise with the help of a weaker observation. Let us introduce for brevity $g(\boldsymbol{r})$ as the Green's function corresponding to a point source located at the origin, $g(\boldsymbol{r}) = G(\boldsymbol{r},\boldsymbol{0})$. A contour plot of $g(\boldsymbol{r})$ in cylindrical coordinates is shown in Fig. 5. The second property to extract from numerical calculation and which is again expected from the interpretation of $g(\boldsymbol{r})$ as potential flow is that $\partial_z g$ has the same sign everywhere. This second property is important because it implies that we can avail ourselves of the absolute values in expression (A4). Using the formulas $\int_0^\infty sK_0(s)\,ds = 1$ and $\sum_{n=1}^\infty \frac{1}{n}\sin(n\alpha) = \frac{\pi-\alpha}{2}$, one finds

$$\max_{z'} \int d^3\boldsymbol{r}\left|\partial_z G\left(\boldsymbol{r},\begin{pmatrix}0\\0\\z'\end{pmatrix}\right)\right| = \int d^3\boldsymbol{r}|\partial_z g(\boldsymbol{r})| = \int d^3\boldsymbol{r}\,\partial_z g(\boldsymbol{r})$$

$$= \int_0^1 dz\sum_{n=1}^\infty \sin(n\pi z) n\int_0^\infty ds 2\pi s K_0(n\pi s) = \frac{1}{2} \tag{A6}$$

so that Eq. (A3) leads to

$$\langle|\partial_z p_1|\rangle \leqslant \tfrac{1}{2}\langle|\boldsymbol{\nabla}\cdot[(\boldsymbol{v}\cdot\boldsymbol{\nabla})\boldsymbol{v}]|\rangle. \tag{A7}$$

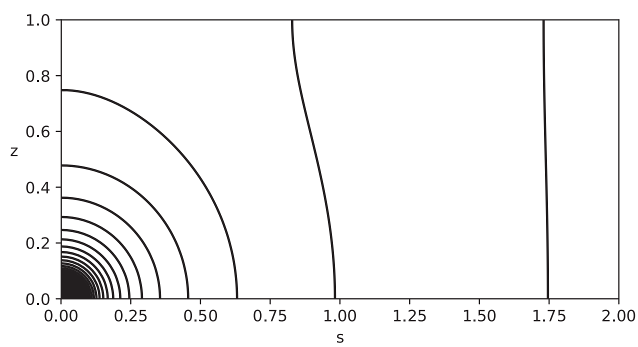

FIG. 5. Contour plot of $g(\boldsymbol{r})$ in a cross section of the layer.

For solenoidal fields $\boldsymbol{v}$, this can be brought into a form which is more pleasant for the SDP:

$$\begin{aligned}\frac{1}{V}\int |\partial_z p_1|\,dV &\leqslant \frac{1}{2}\frac{1}{V}\int \left|\sum_{i,j}(\partial_i v_j)(\partial_j v_i)\right| dV \leqslant \frac{1}{2}\frac{1}{V}\int \sum_{i,j}|\partial_i v_j||\partial_j v_i|\,dV \\ &\leqslant \frac{1}{2}\frac{1}{V}\sum_{i,j}\sqrt{\int (\partial_i v_j)^2\,dV}\sqrt{\int (\partial_j v_i)^2\,dV} \\ &\leqslant \frac{1}{2}\frac{1}{V}\sum_{i,j}\frac{1}{2}\left[\int (\partial_i v_j)^2 dV + \int (\partial_j v_i)^2\,dV\right],\end{aligned} \tag{A8}$$

which in the limit $V \to \infty$ leads to Eq. (23).

[1] L. Howard, Heat transport by turbulent convection, J. Fluid Mech. **17**, 405 (1963).
[2] F. Busse, On Howard's upper bound for heat transport by turbulent convection, J. Fluid Mech. **37**, 457 (1969).
[3] C. R. Doering and P. Constantin, Variational bounds on energy dissipation in incompressible flows: III. Convection, Phys. Rev. E **53**, 5957 (1996).
[4] C. Plasting and G. Ierley, Infinite-Prandtl-number convection. Part 1. Conservative bounds, J. Fluid Mech. **542**, 343 (2005).
[5] C. Seis, Scaling bounds on dissipation in turbulent flows, J. Fluid Mech. **777**, 591 (2015).
[6] I. Tobasco, D. Goluskin, and C. Doering, Optimal bounds and extremal trajectories for time averages in dynamical systems, Phys. Lett. A **382**, 382 (2018).
[7] N. K. Vitanov and F. H. Busse, Bounds on the convective heat transport in a rotating layer, Phys. Rev. E **63**, 016303 (2000).
[8] A. Tilgner, Bounds on poloidal kinetic energy in plane layer convection, Phys. Rev. Fluids **2**, 123502 (2017).
[9] D. Goluskin, Bounding averages rigorously using semidefinite programming: Mean moments of the Lorenz system, J. Nonlinear Sci. **28**, 621 (2018).
[10] S. Chernyshenko, P. Goulart, D. Huang, and Papachristodoulou, Polynomial sum of squares in fluid dynamics: A review with a look ahead, Philos. Trans. R. Soc. A **372**, 20130350 (2014).
[11] G. Fantuzzi, A. Pershin, and A. Wynn, Bounds on heat transfer for Bénard-Marangoni convection at infinite Prandtl number, J. Fluid Mech. **837**, 562 (2018).
[12] N. Balmforth, S. Ghadge, A. Kettapun, and S. Mandre, Bounds on double-diffusive convection, J. Fluid Mech. **569**, 29 (2006).
[13] C. Doering and C. Foias, Energy dissipation in body-forced turbulence, J. Fluid Mech. **467**, 289 (2002).
[14] S. Childress, R. Kerswell, and A. Gilbert, Bounds on dissipation for Navier-Stokes flow with Kolmogorov forcing, Physica D **158**, 105 (2001).
[15] B. Rollin, Y. Dubief, and C. Doering, Variations on Kolmogorov flow: Turbulent energy dissipation and mean flow profiles, J. Fluid Mech. **670**, 204 (2011).
[16] A. Tilgner, Scaling laws and bounds for the turbulent G. O. Roberts dynamo, Phys. Rev. Fluids **2**, 024606 (2017).
[17] S. Chernyshenko, Relationship between the methods of bounding time averages, arXiv:1704.02475.
[18] J. Jackson, *Classical Electrodynamics*, 3rd ed. (Wiley, New York, 1999).